Texture Change of Ice on Anomalously Preserved Methane Clathrate Hydrate

Wataru Shimada, Satoshi Takeya,* Yasushi Kamata, Tsutomu Uchida,† Jiro Nagao, Takao Ebinuma, and Hideo Narita

National Institute of Advanced Industrial Science and Technology (AIST), Tsukisamu-Higashi, Sapporo 062-8517, Japan

Received: November 25, 2004; In Final Form: January 20, 2005

We used a confocal scanning microscope to observe growth and texture change of ice due to the dissociation of methane gas clathrate hydrate (CH_4 hydrate). The experiments were done under CH_4 gas atmospheric pressure and isothermal conditions between 170 and 268 K. Above 193 K, the dissociation of CH_4 hydrate resulted in many small ice particles that covered the hydrate surface. These ice particles had roughly the same shape and density between 193 and 210 K. In contrast, above 230 K the ice particles developed into a sheet of ice that covered the hydrate surface. Moreover, the measured release of CH_4 gas decreased when the sheet of ice formed at the surface of the hydrate. These findings can explain the anomalous preservation behavior of CH_4 hydrate; that is, the known increase of storage stability of CH_4 hydrate above 240 K is likely related to the formation of the ice that we observed in the experiments.

Introduction

Gas hydrates are ice-like inclusion compounds formed from water and gas molecules under high pressures and low temperatures that contain a high density of gas. The actual gas storage density depends on the gas occupation fraction in the hydrate and the particular crystallographic structure of the hydrate.[1−4] Nevertheless, a given volume of gas hydrate contains more than 150 times the mass of gas as that for the same volume of pure gas at standard temperature and atmospheric pressure. For this reason, CH_4 hydrate is expected to become a new energy source[5] and also a medium for energy storage and transport.[6] Provided the temperature is below 273 K, CH_4 hydrate can be stored at atmospheric pressure even though such a condition allows dissociation.

It was found that CH_4 hydrate and ice could be stored at atmospheric pressure and 267 K for two years, and this phenomenon was then named self-preservation[7] because the dissociation temperature of CH_4 hydrate under atmospheric pressure is about 193 K.[1] Takeya et al.[8,9] measured the dissociation of powdered CH_4 hydrate below 253 K using time-resolved X-ray diffraction and concluded that the dissociation rate is controlled by the rate of gas diffusion through ice below 198 K, which is a temperature region where the dissociation pressure of CH_4 hydrate is lower than 0.1 MPa CH_4 gas atmospheres. Recently, Komai et al.[10] estimated the diffusion coefficient of CH_4 in the ice coating around CH_4 hydrate using Raman spectroscopy and found it to be the same order of magnitude as the theoretical diffusion coefficient of CH_4 in hexagonal ice at the temperatures from 268.2 to 272.7 K. These studies based on crystal structure transition clarified that the dissociation rate is controlled by the rate of gas diffusion through ice. However, one remaining puzzle is the anomalous preservation behavior of massive CH_4 hydrate samples in which the storage stability of CH_4 hydrate between 242 and 271 K is greater than that below 240 K.[11] On the other hand, the experimental results of CO_2 hydrate, type I structure, and methane (CH_4) + ethane (C_2H_6) mixed gas hydrate, type II structure, did not show identical anomalous preservation behavior with CH_4 hydrate, whereas its dissociation pressure is lower than that of CH_4 hydrate at the same temperature conditions.[12,13] Circon et al.[12] also showed that CO_2 hydrate samples release only 3% of their gas content by isobaric slow warming up to 240 K, which is 22 K above the hydrate phase boundary. These conflicts of hydrate dissociation behaviors suggest the potential roles of ice in the self-preservation effect. For example, a recent report by Kuhs et al. suggests the relation between anomalous preservation and stacking-fault of ice due to transformations from cubic ice to hexagonal ice.[14]

In this paper, we focus on texture changes of ice during the dissociation process of CH_4 hydrate because the texture of ice crystals affects its physical properties. We report in situ observations of the surface of CH_4 hydrate samples during dissociation under 0.1 MPa CH_4 gas atmospheres. We found that above 230 K, a texture change of the CH_4 hydrate surface occurs and the amount of gas released from CH_4 hydrate decreases dramatically. On the basis of these results, we discuss the mechanism of self-preservation during dissociation of CH_4 hydrate.

Experimental Section

We used a batch-type reactor at 274 K and 5.0 MPa to grow CH_4 hydrate specimens from 99.95% pure CH_4 and distilled H_2O of conductivity 0.06 μS/cm. Details of this reactor are in Uchida et al.[15] After the hydrate formed, the reactor was cooled below 100 K and then the remaining gas was released at a temperature of approximately 100 K. We removed the hydrate samples from the reactor, and only those specimens that looked like single grains of CH_4 hydrate of about 5-mm diameter were chosen for our experiments. This processing was done under an N_2 gas atmosphere below 100 K.

A confocal scanning microscope (CSM, Lasertec model 1HD200) was used to observe surface changes as a CH_4 hydrate

* Corresponding author. Present address. RIFF, AIST, Central 5, Higashi 1-1-1, Tsukuba 305-8565, Japan. E-mail: s.takeya@aist.go.jp

† Present address. Graduate School of Engineering, Hokkaido University, N13W8 Sapporo, 060-8628, Japan

10.1021/jp044624t CCC: $30.25 © 2005 American Chemical Society
Published on Web 03/03/2005

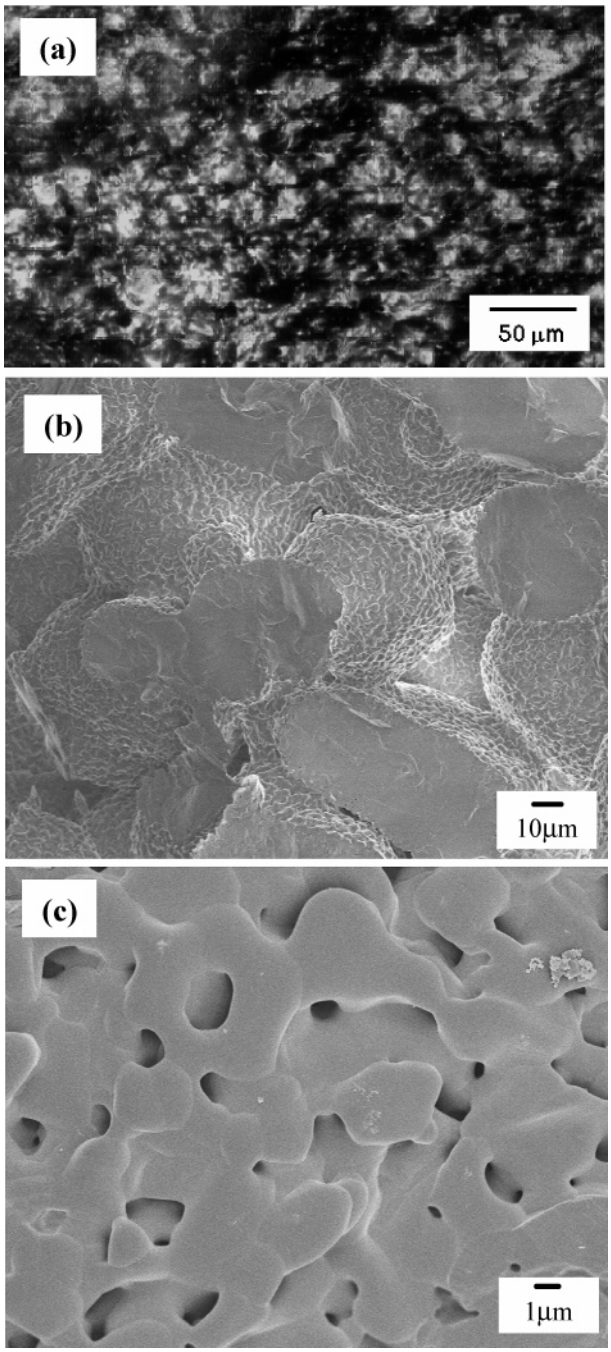

Figure 1. Surface image of the CH_4 hydrate grown at 274 K and 5.0 MPa using a batch-type reactor. (a) CSM images of the CH_4 hydrate surface at 170 K under 0.1 MPa CH_4 gas pressure atmospheres. White regions are flat or smooth surface regions, whereas dark regions are concave or the other side of particles and domains that scatter all of the light. (b) FE-SEM images of the CH_4 hydrate surface at 93 K. Larger-scale view. The smooth sections were likely caused by the cutting of the sample with a cold knife in the cryo-preparation chamber. (c) Enlarged image of (b).

sample dissociated. Three-dimensional data can be recorded by the CSM due to scanning objects and suppression of out of focus structure. It took three minutes to record the images. A digital camera (Nikon Coolpix 4500) connected to time-lapse VTR was attached to the CSM for real-time observations. One grain of sample was put into a cryo-cell equipped with the CSM and kept under 170 K and 0.1 MPa CH_4 gas atmospheres during each observation. By this method, we could directly observe changes in the hydrate surface at atmospheric pressure, while the observations using a scanning electron microscope (SEM)

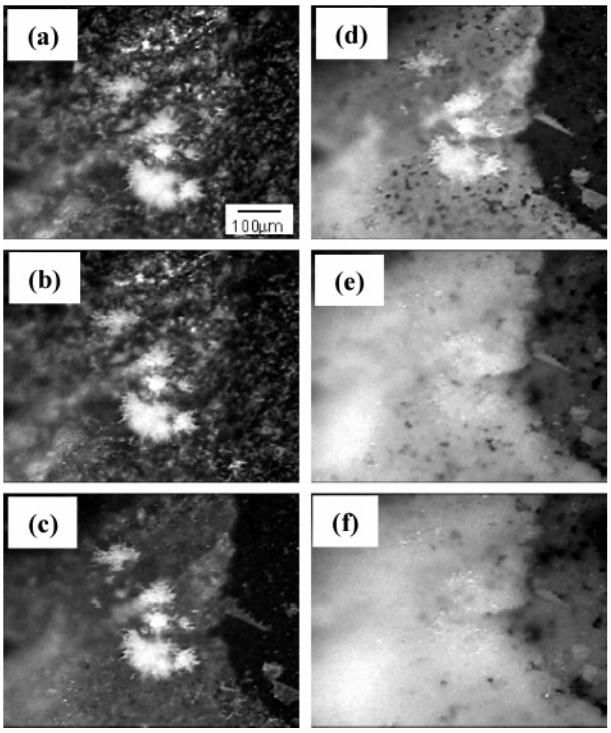

Figure 2. Real-time images taken with a digital camera as the temperature increased at 5 K/min. (a) 170 K, (b) 180 K, (c) 190 K, (d) 200 K, (e) 210 K, and (f) 220 K. The cloudy structures in (d−f) are due to the surface being covered by many small ice particles. In (a−d), the large white sections near the center of the images are ice frost-flowers.

can be done only under vacuum conditions where hydrate crystals are not stable. The temperature was measured using a thermocouple in the cryo-cell, and the temperature deviation between atmospheric temperature in the cryo-cell and that of sample surfaces was within 1 K above 230 K.

During the CSM surface observations, we measured the amount of CH_4 gas released from the dissociating hydrate in the cryo-cell. The cryo-cell was connected to a water bath, and the gas flow was measured by collecting gas released from the dissociating samples. The temperature of the hydrate was increased by 5 K/min continuously from 170 K to a designated temperature from 200 to 268 K. Then the temperature was kept at this designated temperature for 90 min. Finally, the temperature was increased by 5 K/min continuously up to 279 K.

We also used a field emission scanning electron microscope (FE-SEM; JEOL model HF-JSM6700F) equipped with cryo transfer system (Gatan model Alto2100), which enabled us to observe the sample surface below 90 K without dissociation. The image was used to confirm the surface structure of the CH_4 hydrate sample synthesized with the batch-type reactor.

Results and Discussion

The images in Figure 1a show a sample hydrate made using the batch-type reactor, which was kept at 170 K using CSM under 0.1 MPa CH_4 gas atmospheres. The images show the structure just before a dissociation experiment. The surface of the hydrate sample appears to have small size particles. A sample hydrate was also measured by FE-SEM under vacuum conditions, and the hydrate sample appears to be an aggregate of roughly spherical-shaped particles of several tens of micrometers in diameter (Figure 1b). Further magnification shows each particle to itself be an aggregate of even smaller particles

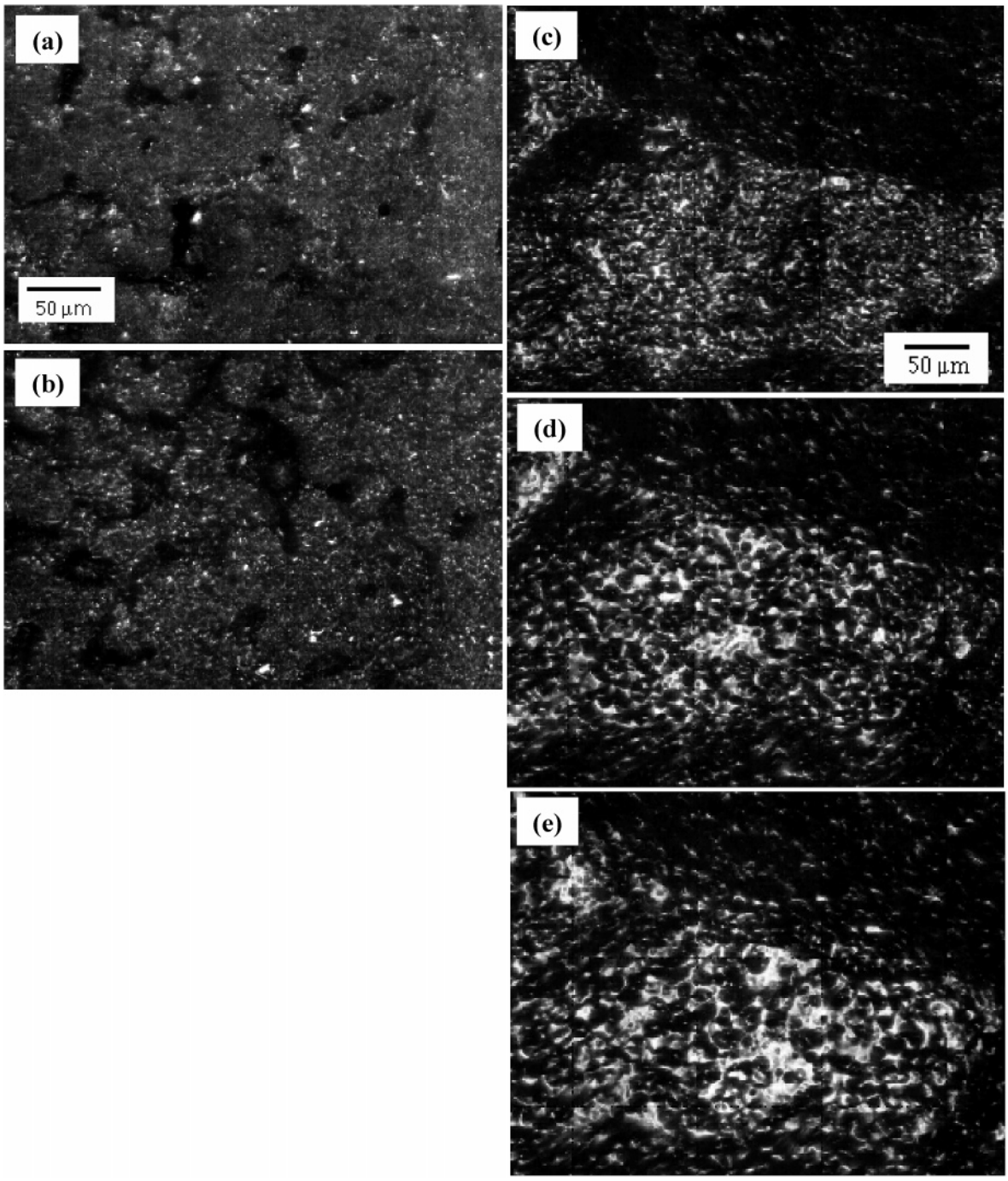

Figure 3. CSM images of the CH_4 hydrate surface at (a) 200 K and (b) after keeping the temperature constant for 90 min, while at (c) 250 K, (d) after keeping the temperature at 250 K for 40 min, and (e) after keeping at 250 K for 80 min. White regions are flat or smooth surface regions, whereas dark regions are concave or the other side of particles and domains that scatter all of the light.

(Figure 1c). This texture is different from the submicron porous structure reported previously for CH_4 hydrate.[13,16] The different texture is likely related to the different methods used to make the hydrate. We made the hydrate sample from a mixture of liquid water and CH_4 gas, whereas the submicron porous hydrate was made from ice and CH_4 gas. With liquid water and CH_4 gas, small CH_4 hydrate particles would nucleate and then agglomerate during stirring.

As the temperature increased, the surface texture of the hydrate changed. Figure 2 shows real-time observations by the time-lapse VTR how the hydrate surface changed with temperature. Below 180 K, the surface change was not observed. Above 190 K, the increasing rapidity of the dissociation resulted in an increasing amount of small particles on the surface. The small particles were suggested to be hexagonal ice, not CH_4 hydrate, by the X-ray diffraction method.[17] The number density of ice becomes so large that the surface looks cloudy. At 220 K (Figure 2f), the surface is completely covered with ice particles.

As the time passed, the surface texture of the hydrate changed even at constant temperatures. CSM images show detailed surface structures of CH_4 hydrate. At 200 K, most of the surface appears to be covered by small ice particles and there are some concaves which would be paths for CH_4 gas release from the dissociating hydrate (Figure 3a). The surface texture of the sample did not change at 200 K even after 90 min (Figure 3b). At 250 K, the surface was also covered by ice particles, but each particle size of ice looks larger than those of 200 K due to

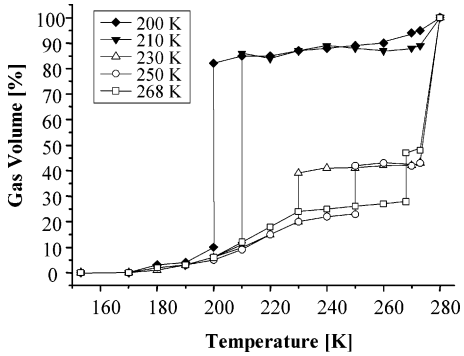

Figure 4. Released CH_4 gas during dissociation of hydrate. 100% means all of the gas in the sample. Each curve is for a different designated temperature (in the legend) at which the sample was held for 90 min. Before and after the holding temperature, the temperature was raised at 5 K/min.

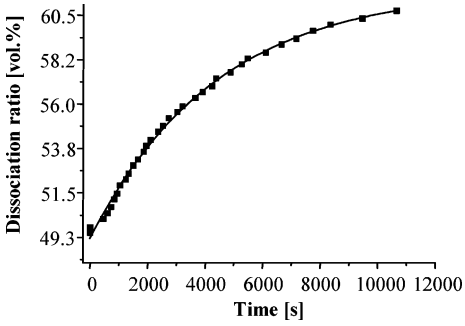

Figure 5. Time change of released CH_4 gas during dissociation of hydrate at 250 K. The volume ratio of CH_4 hydrate at initial time at 250 K was 49.5%, when sample temperature was increased up to 250 K. The fitting curve is expressed as $y = 0.6181 - 0.1258 \times 0.9998^x$.

the growth of each ice particles (Figure 3c). After 80 min, the texture changed into a dense sheet of ice with a domain size, which suggests grain size of ice composing sheet of ice, of several tens of micrometers at 250 K (Figure 3e).

At the same time, we measured the amount of CH_4 gas released from the dissociating hydrate in the cryo-cell for five such designated temperatures (Figure 4). Above approximately 190 K, the hydrate started to dissociate. In the cases that 200 and 210 K were the designated temperatures, more than 80% of storage gas in the hydrate was released during the 90-min wait. On the other hand, above 230 K, the amount of released CH_4 gas during the 90-min wait was approximately only 20%, and most gas was released when the ice melted. These results show that the dissociation rate of CH_4 hydrate was suppressed above 230 K due to the sheet formation of ice. Figure 5 shows time change of the amount of released CH_4 gas for 180 min at 250 K. The figure shows that the dissociation rate decreased with time.

These surface changes of CH_4 hydrate due to the dissociation can be explained by the following mechanism. Some hydrate dissociates, H_2O from dissociation transforms directly to ice. At the same time, both H_2O and CH_4 are likely to evaporate into the surrounding space because direct transformation from solid to solid, such as hydrate to ice, would not be an easy process. The continued dissociation cools the surface and supersaturates the H_2O vapor pressure. Then H_2O condenses as frost on the hydrate surface because the surface temperature would be colder than the controlled atmospheric temperature due to endothermic hydrate dissociation reaction (see Figure 6a). Hexagonal ice reaches equilibrium with the vapor and then becomes smooth as the sharp frost points evaporate and condense in concave regions (see Figure 6b). This evaporation-condensation type of sintering would be faster at higher temperatures, especially above 230 K because the vapor pressure of ice increases drastically above around 230 K, assuming that the vapor pressure of ice under CH_4 atmosphere is similar to that of air.[18] The apparent ice patches in Figure 3e do not show a complete ice sheet such as previously reported by Stern et al.,[13] while the texture is consistent with previous observations by Kuhs et al.[15] The formation of a complete sheet of ice should take much longer than 90 min; nevertheless, the surface appears to be forming a sheet of ice as the ice domains in Figure 3e are large as those in Figure 3c. The sheet of ice at the surface of the hydrate would reduce the rate of CH_4 gas release from the dissociating hydrate by sealing the surface of the hydrate.

Here, we estimate the sealing effect for self-preservation by spherical hydrate dissociation model from refs 9 and 10. Heat flow from the temperature-controlled cryo-cell to the reaction boundary is fast, and thus the temperature depression due to the endothermic dissociation reaction on the hydrate should be negligible (see Figure 6c). In the model, the outermost layer is ice with an outside radius r_i. This ice layer likely consists of ice particles as in Figure 3a or 3c. The internal sphere is hydrate with radius r_h ($< r_i$). The CH_4 gas that is released from the dissociating hydrate should build up in the region between the hydrate and the ice until the pressure is nearly equal to the dissociation pressure of CH_4 hydrate. Thus, the hydrate should remain close to equilibrium. Then, some parts of the external ice sphere would likely fracture above 193 K because the dissociation pressure is higher than atmospheric pressure.[1] Thus, significant amounts of hydrate can dissociate, and CH_4 gas escapes through the cracks. On the other hand, once the ice particles sinter into a sheet of ice (see Figure 3e), the ice layer can withstand the pressure difference between internal dissociation pressure of CH_4 hydrate and atmospheric pressure mechanically. The dissociation rate is much lower in this case. From the above model, the mechanical properties of the sheet of ice are now addressed quantitatively. The normal stress σ_r, which is perpendicular to the sheet of ice, and the tangential stress σ_t, which is parallel to the tangent of sheet of ice, are[19]

$$\sigma_r = \frac{p_a r_i^3 (r^3 - r_h^3)}{r^3 (r_h^3 - r_i^3)} + \frac{p_d r_h^3 (r_i^3 - r^3)}{r^3 (r_h^3 - r_i^3)} \quad (1)$$

$$\sigma_t = \frac{p_a r_i^3 (2r^3 + r_h^3)}{2r^3 (r_h^3 - r_i^3)} - \frac{p_d r_h^3 (2r^3 + r_i^3)}{2r^3 (r_h^3 - r_i^3)} \quad (2)$$

Here, r is a radius such that $r_h \le r \le r_i$, p_d is the dissociation pressure of CH_4 hydrate, and p_a (= 0.1 MPa) is atmospheric pressure. In the present study, about 55% of the CH_4 hydrate remained even after holding the temperature constant at 250 K for 90 min (Figure 4). Assuming that the external radius of ice r_i is equal to that of initial hydrate (~2.5 mm), then the remaining hydrate radius r_h would be 2.0 mm. The dissociation pressure of CH_4 hydrate p_d at 250 K is about 1.3 MPa.[1] Then the maximum normal stress is estimated to be 1.3 MPa at $r =$ 2.0 mm, and the maximum tangential stress is estimated to be 2.4 MPa at $r = 2.0$ mm. On the other hand, the reported stress of polycrystalline ice was about 1.2 MPa with 1.0 mm domain size of ice at 10^{-6} s^{-1} strain rate and 253 K.[18] Then the strength is weaker than the estimated tangential stress value of 2.4 MPa in this study. However, the tensile strength σ of polycrystalline ice composed of ice domains with diameter d [m] is $\sigma = 0.60 + 0.02d^{-0.51}$ MPa at 10^{-6} s^{-1} strain rate.[20] Thus, the tensile strength increases with decreasing domain size of ice. Assuming

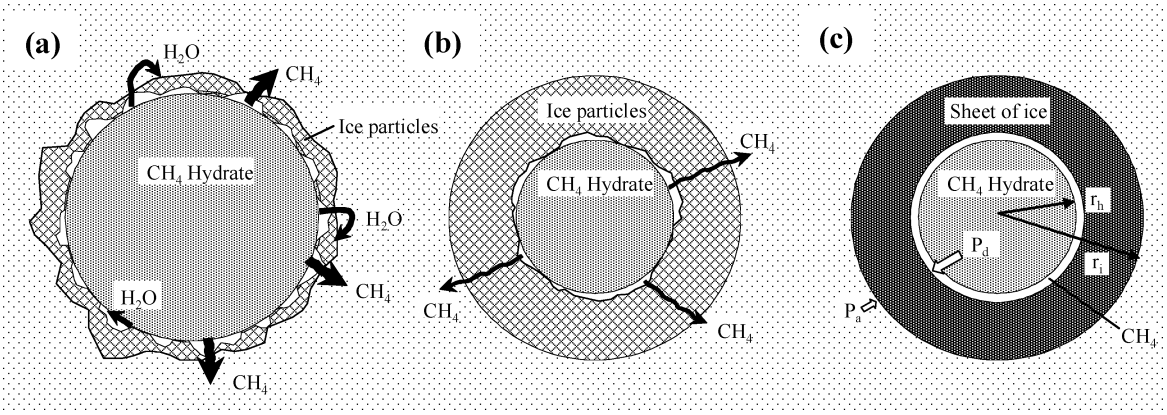

Figure 6. A sketch showing our assumed model for the transformation of CH_4 hydrate to ice under 0.1 MPa CH_4 gas atmospheres. (a) H_2O condensed as frost on a hydrate surface and CH_4 likely evaporate into surrounding apace. (b) Hexagonal ice reaches equilibrium with the vapor and then becomes smooth as the sharp frost points evaporate and condense in concave regions. (c) Outer ice particles changed into a sheet of ice. Here r_i (~2.5 mm) is the external radius of the ice layer and r_h is the external radius of the hydrate.

that this equation for tensile stress and the domain size of ice can be extrapolated down to 10 μm (to allow us to use the domain sizes in Figure 3d), the strength of ice was estimated to be 7.7 MPa and exceed the estimated value of 2.4 MPa in this study. In this case, it is possible to prevent further dissociation by the mechanical sealing of the sheet of ice.

Next, we estimate the dissociation ratio of CH_4 hydrate quantitatively. By fitting the data of Figure 5 and differentiating the fitting equation, we calculated dissociation rates at initial time, when sample temperature was increased up to 250 K, and after 180 min. As a result, the dissociation rates of 2.5×10^{-3} vol %/s at the initial time and 2.1×10^{-3} vol %/s after 180 min were estimated. These values are in good agreement with the previous results by Stern et al.[11] We also estimate the CH_4 gas diffusion for self-preservation by the above spherical hydrate dissociation model. Assuming that the external radius of ice is equal to that of initial hydrate and that the external radius of the entire particle is constant, $r_i = r_{ho}$,

$$3(1-R^2) + 2(R^3 - 1) = \frac{6D}{r_{ho}^2} k(P_d(T) - P_a)t \qquad (3)$$

Here, R is the scaled radius of the hydrate and D is the diffusion coefficient of CH_4 gas through ice layer. $R = r_h/r_{ho}$. P_d (T) is the dissociation pressure of CH_4 gas in at temperature T, P_a is the pressure of CH_4 gas in the surrounding atmosphere, and k is constant because gas flux in the sheet of ice would be proportional to the pressure difference of the CH_4 gas. Therefore, if diffusion of CH_4 gas through ice layer at constant diffusion coefficient being the rate-limiting step is valid, a plot of $3(1-R^2) + 2(R^3-1)$ vs t would be a straight line with slope equal to the factors of t on the right side of eq 3. However, Figure 7 suggests that the dissociation of CH_4 hydrate at 250 K is not rate controlled by the CH_4 gas diffusion through the sheet of ice at constant diffusion coefficient, except in the initial 30 min, approximately. It suggests that the diffusion coefficient decreased as time passed. This result is in good agreement with our observed result because growth of each ice domain will suppress CH_4 gas diffusion through boundaries.

The experimental results in this study suggest the following self-preservation mechanism for CH_4 hydrate under a 0.1 MPa CH_4 gas atmosphere. Below 193 K, the dissociation pressure of CH_4 hydrate is lower than atmospheric pressure, thus CH_4 hydrates are stable. Above 193 K and below about 230 K, the dissociation rate may be controlled by the rate of CH_4 hydrate dissociation because CH_4 gas diffuses easily through the frost-like ice particle layer due to pressure difference between the dissociation pressure and atmospheric pressure. Accordingly, the dissociation rate should increase as the temperature increases in this temperature range. Above about 230 K, the small ice particles change into a dense ice layer due to sintering of ice; the dense ice layer seals the CH_4 hydrate. As a result, the dissociation rate is suppressed and controlled by the rate of CH_4 gas diffusion in ice crystals.

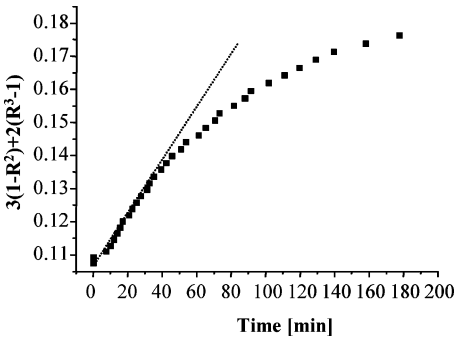

Figure 7. Diffusion-controlled dissociation model. The ordinate is a function of the scaled hydrate radius R that appears in the diffusion eq 1. A dotted straight line indicates that dissociation was controlled by CH_4 diffusion through a sheet of ice at constant diffusion coefficient.

Conclusion

To better understand the self-preservation effect for small particles of CH_4 hydrate, we observed the ice crystals which grew on the CH_4 hydrate surface during dissociation at various temperatures and measured the amount of released gas. Above 193 K, the surface became covered by small ice particles as the CH_4 hydrate dissociated. Above 230 K, these small ice particles grew and merged into a sheet of ice with a grain size of several tens of micrometers that hindered the dissociation of CH_4 hydrate. We observed the formation of this sheet only at 230 K and higher temperatures and argued that the resulting sheet of ice sealed the dissociating hydrate. Thus, these observations should help explain the anomalous preservation effect of CH_4 hydrate.

Acknowledgment. We thank R. Ohmura and S. Jin of AIST for their discussions with us, and we also thank N. Kikuchi of LEOL Ltd. and M. Carey of Gatan UK for their support of our measurements. S.T. thanks T. Hondoh and J. Okuyama of

Hokkaido University and J. Nelson for their comments on ice properties. This work was supported by the Research Consortium for Methane Hydrate Resources in Japan (MH21 Research Consortium) and Japan Science and Technology Corporation (JST).

References and Notes

(1) Sloan, E. D. *Clathrate Hydrate of Natural Gases*, 2nd ed.; Marcel Dekker: New York, 1998.
(2) Müller, H. R.; Stackelberg, M. V. *Naturwissenschaften* **1952**, *39*, 20.
(3) Stackelberg, M. V.; Müller, H. R. *Naturwissenschaften* **1951**, *38*, 456.
(4) Ripmeester, J. A.; Tse, J. S.; Ratcliffe, C. I.; Powell, B. M. *Nature* **1987**, *325*, 135.
(5) Kvenvolden, K. A. *Natural Gas Hydrate in Oceanic and Permafrost Environments*; Max, M. D., Ed.; Kluwer Academic Publishers: Dordrecht, 2000.
(6) Gudmundson, J.; Borrehaug, A. *Proceedings of the 2nd International Conference on Natural Gas Hydrates*; Monfort, J. P., Ed.: Toulouse, 1996; p 415.
(7) Yakushev, V. S.; Istomin, V. A. *Physics and Chemistry of Ice*; Hokkaido University Press: Sapporo, 1992; p 136.
(8) Takeya, S.; Shimada, W.; Kamata, Y.; Ebinuma, T.; Uchida, T.; Nagao, J.; Narita, H. *J. Phys. Chem. A* **2001**, *105*, 9756.
(9) Takeya, S.; Ebinuma, T.; Uchida, T.; Nagao, J.; Narita, H. *J. Cyst. Growth* **2002**, *237*−*239*, 379.
(10) Komai, T.; Kang, S.; Yoon, J.; Yamamoto, Y.; Kawamura, T.; Ohtake, M. *J. Phys. Chem. B* **2004**, *108*, 8062.
(11) Stern, L. A.; Circone, S.; Kirby, S. H.; Durham, W. B. *J. Phys. Chem. B* **2001**, *105*, 1756.
(12) Circone, S.; Stern, L. A.; Kirby, S. H.; Durham, W. B.; Chakoumakos, B. C.; Rawn, C. J.; Rondinone, A. J.; Ishii, Y. *J. Phys. Chem. B* **2003**, *107*, 5529.
(13) Stern, L. A.; Circone, S.; Kirby, S. H.; Durham, W. B. *Can. J. Phys.* **2003**, *81*, 271.
(14) Kuhs, W. F.; Genov, G.; Satykova, D. K.; Hansen, T. *Phys. Chem. Chem. Phys.* **2004**, *6*, 4917.
(15) Uchida, T.; Hirano, T.; Ebinuma, T.; Narita, H.; Gohara, K.; Mae, S.; Matsumoto, R. *AIChE J.* **1999**, *45*, 2641.
(16) Kuhs, W. F.; Klapproth, A.; Gotthardt, F.; Techmer, K.; Heinrichs, T. *Geophys. Res. Lett.* **2000**, *27*, 2929.
(17) Takeya, S.; Uchida, T.; Nagao, J.; Ohmura, R.; Shimada, W.; Kamata, Y.; Ebinuma, T.; Narita, H. *Chem. Eng. Sci.* **2005**, *60*, 1383.
(18) Petrenko V. F.; Whitworth, R. W. *Physics of ice*; Oxford University Press: New York, 1999.
(19) Timoshenko, S.; Goodier, J. N. *Theory of elasticity*, 3rd ed.; McGraw-Hill Education: New York, 1970.
(20) Currier, J. H.; Schulson, E. M. *Acta Metall.* **1982**, *30*, 1511.